IOPscience iopscience.iop.org

Home Search Collections Journals About Contact us My IOPscience

Localization on continuous random networks in two dimensions: a numerical study

This article has been downloaded from IOPscience. Please scroll down to see the full text article.

1992 J. Phys.: Condens. Matter 4 1093

(http://iopscience.iop.org/0953-8984/4/4/019)

View the table of contents for this issue, or go to the journal homepage for more

Download details:
IP Address: 171.66.16.159
The article was downloaded on 12/05/2010 at 11:09

Please note that terms and conditions apply.

J. Phys.: Condens. Matter 4 (1992) 1093–1102. Printed in the UK

Localization on continuous random networks in two dimensions: a numerical study

Th Koslowski and W von Niessen

Institut für Physikalische und Theoretische Chemie, Technische Universität Braunschweig, D-3300 Braunschweig, Federal Republic of Germany

Received 9 July 1991

Abstract. We report numerical results for localization induced by disorder on a continuous random network. A simple tight-binding model and a Hamiltonian with off-diagonal disorder are used to calculate the localization properties of electronic states. For both models, localization occurs at the upper band edge. In addition, off-diagonal disorder leads to localization at the lower band edge. For both models the density of states, mobility edges and localization lengths have been calculated, leading to significant differences. We discuss the possibility of extending the model to systems in three dimensions, like amorphous semiconductors.

1. Introduction

In solid state theory, several models have been established to study the properties of disordered systems. They can be described by the geometry of the system, usually based on a regular lattice, and by a tight-binding Hamiltonian reading

$$\hat{H} = \sum_i \epsilon_i \hat{c}_i^+ \hat{c}_i + \sum_{j \neq i} V_{ij} \hat{c}_i^+ \hat{c}_j \tag{1}$$

where $\hat{c}_i$ and $\hat{c}_i^+$ are creation and annihilation operators operating on the space of atomic orbitals $|i\rangle$ located at the lattice sites. The basis is assumed to be orthogonal.

In the original Anderson model (Anderson 1958), the diagonal elements of the Hamiltonian can vary uniformly from $-W/2V$ to $+W/2V$, wheras the interaction V_{ij} is a constant between nearest neighbours. Due to a fundamental theorem of Anderson (1958) all eigenfunctions of a disordered system become localized if the disorder exceeds some specific value W_c. For a given value $W < W_c$ the density of states can be divided into a part where all states are localized and into another part containing extended states only. These are separated by a mobility edge E_c (Ziman 1969, Mott and Davis 1971). This behaviour has also been observed in systems with off-diagonal disorder (Gibbons *et al* 1988) or in the quantum percolation problem (Soukoulis *et al* 1987, Koslowski and von Niessen 1990, 1991). The existence of localized states has a tremendous influence on zero degree transport properties. As charge transport between localized states is only allowed by phonon assisted hopping, requiring a non-zero temperature, systems exhibiting localized states at the Fermi energy become insulators in the limit $T \to 0$ K.

0953-8984/92/041093+10$04.50 © 1992 IOP Publishing Ltd

Disordered systems with covalent bonds like amorphous silicon and other tetrahedrally coordinated amorphous semiconductors can be described by a continuous random network (CRN). Within this network, each atom has the same coordination number Z as in the crystalline solid, but long range topological order is destroyed. Distortions of bond lengths and angles from the values of crystalline solids are small. The properties of a hand-build model almost fulfilling these conditions has been constructed by Polk for the first time (Polk 1971). It is widely accepted that amorphous solids show localized states at the band edges (Elliott 1983), so the question whether CRNs will also exhibit this feature arises almost automatically.

In this article we present a quantitative calculation of the localization properties of the eigenstates of a simple CRN. Due to the scaling theory of localization, localized eigenstates will be favoured by a small Euclidean dimension D. As $D = 2$ is the smallest possible dimension that allows topological disorder, we have constructed a CRN derived from the square lattice. The role of topological disorder will be studied by using a nearest neighbour tight-binding Hamiltonian. To study the influence of bond length variation, a Hamiltonian with a r-dependent potential is used. In order to generate a continuous bond length distribution, the CRN has been relaxed by a Monte Carlo method, using the Keating potential (Keating 1966). The scheme presented here can be applied to three-dimensional systems, including the diamond lattice.

In the following section we describe the method of constructing a CRN, the relaxation procedure and the model Hamiltonians. A detailed description of the way localization properties are obtained will be given. Results are reported in section 3, with a special emphasis on charge transport at low temperatures. The influence of different model Hamiltonians on localization properties is discussed, we give an outlook onto three dimensional systems. In section 4, conclusions of the work reported in this article will be given.

2. Methods

There are numerous ways of constructing a CRN, including hand build, computer modified and computer generated models (Elliott 1983, Duffy *et al* 1974). For our calculation of localization on a CRN, the model should fulfil the following requirements: (a) it has to be generated easily on a computer, saving computer time and allowing a large number of realizations; (b) no dangling bonds should be included, so the model represents an idealized amorphous solid without any additional defects; (c) each atom should be surrounded by four nearest neighbours, regardless of its position, so cyclic boundary conditions have to be imposed. We decided to use the vacancy model of Duffy and co-workers (Duffy *et al* 1974), which fulfils all of the requirements mentioned above.

On a square lattice, each atom is surrounded by four nearest neighbours (left = l, right = r, top = t, bottom = b). Whenever it is decided to eliminate an atom, two new bonds will be created, symbolized by a simple line (–). There are two ways of connecting the neighbours of the vacancy without bond crossing. Either a (t–r)-bond and a (b–l)-bond or a (t–l)-bond and a (b–r)-bond may be formed. In our realization of the model, each configuration may appear with probability 1/2. For a specific vacancy, the actual bond configuration is chosen randomly. To avoid the formation of double bonds, no neighbour of a vacancy can be changed into a vacancy. Only atoms

showing an even column index and an even row index have been taken into account as a vacancy candidate, so this problem is avoided automatically. The probability p of changing a vacancy candidate into a vacancy is chosen as the disorder parameter of the model. To obtain the actual vacancy rate, p has to be divided by a factor of four. The elimination of an atom leads to the creation of two three-membered rings and one six-membered ring, erasing four four-membered rings. To illustrate the topology of a network created in this way, a 20×20 lattice is shown in figure 1 ($p = 0.4$). Although the lattice has been relaxed, the topology is the same as it is in the unrelaxed case.

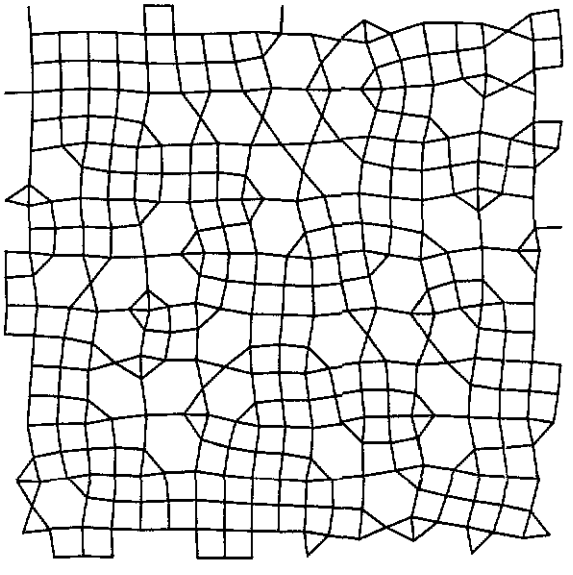

Figure 1. Continuous random network, 20×20, $p = 0.4$, after 400 Monte Carlo steps.

The procedure of creating a CRN as described above introduces additional strain to the lattice. In any real lattice, the large distortions in bond lengths and bond angles will lead to a relaxation of the lattice. For this relaxation, we use the well known Keating potential (Keating 1966)

$$U_i = \frac{3\alpha}{16R_0^2}\sum_{i\neq j}(R_{ij}^2 - R_0^2)^2 + \frac{3\beta}{8R_0^2}\sum_{i(j,k)}(R_{ji}\cdot R_{ki} + \tfrac{1}{3}R_0^2)^2 \qquad (2)$$

with $R_{ij} = |r_i - r_j|$, $\alpha/\beta = 3$, which corresponds to the Keating parameters for amorphous silicon. The second sum spans all distinct pairs of neighbours of i. The first term in equation (2) describes an atom–atom interaction, the second term a bond–bond interaction. For each realization, the length scale has been changed in a way that the average nearest neighbour distance R_0 of the disordered systems equals R_0 of the crystalline system, ensuring that the amorphous phase has the same density as the crystalline phase. To look for a potential energy minimum, we have used a Monte Carlo method. For a system containing n atoms, n Monte Carlo steps have

been performed. On the average, the attempt to move each atom has been made once for every Monte Carlo step. The maximum atomic displacement has been set to one tenth of R_0, the temperature has been set to zero. So an attempt to move an atom has only been put into effect if it had caused a decrease in energy. As the change in energy due to moving an atom can be calculated from a local configuration, the Monte Carlo relaxation can be performed very efficiently. It should be noted that a broad distribution of the bond angle persists after the relaxation has been performed. As both the tight-binding Hamiltonian and the extended Hückel Hamiltonian described below do not include any angle-dependent terms, this distribution of bond angles does not introduce any additional disorder.

Two model Hamiltonians are used for the calculation of the electronic properties of the system. The first model is a simple nearest neighbour tight-binding model. In equation (1), V_{ij} equals $1/Z$ if i and j are nearest neighbours, V_{ij} equals zero else. In the second model, V_{ij} is a function of distance:

$$V_{ij}(R) = V_0(1 + bR + \tfrac{1}{3}b^2R^2)\mathrm{e}^{-bR}\Theta(\tfrac{5}{2}bR_0 - bR) \tag{3}$$

where b is a gauge factor, which guarantees that $V_{ij}(R_0) = 1/4$. So the nearest neighbour matrix element of the simple tight-binding Hamiltonian equals the matrix element of the Hamiltonian described by equation (3), taken at the point of average nearest neighbour distance R_0. Equation (3) is related to extended Hückel theory (Hoffmann 1963) where the elements of the Hamiltonian matrix are proportional to the matrix elements of the overlap matrix. In the case of the above Hamiltonian, the overlap integral S has been calculated for two hydrogen atomic orbitals $S = \langle 1\mathrm{s}_i|1\mathrm{s}_j\rangle$. The Heavyside function $\Theta(\frac{5}{2}bR_0 - bR)$ forces a cut-off in V at distances larger than twice the average nearest neighbour distance, so the Hamiltonian matrix remains sparse. The diagonal energy ϵ of equation (1) is taken as zero in both models.

To study the localization properties of the CRN, we use the TEL method of Thouless, Edwards and Licciardello (Edwards and Thouless 1972, Licciardello and Thouless 1975, 1978). These authors have been able to show that the energy shift ΔE caused by a change in boundary conditions is related to the conductivity of the system

$$\sigma(L) = (e^2/2\hbar)L^{2-D}\,\Delta E(L)/\delta E(L) \tag{4}$$

L is the system length, D its Euclidean dimension and δE the average spacing of the energy levels. In practice, ΔE and δE are averages within a certain energy interval. Due to its large fluctuations, ΔE is usually taken as a geometric mean. The scaling behaviour of $\sigma(L)$ has been used by several authors to study the Anderson problem on a large variety of lattices, (Licciardello and Thouless 1975, 1978). Localization properties in a magnetic field and under the influence of spin-orbit coupling (Ando 1988, 1989) or the quantum percolation problem (Koslowski and von Niessen 1990, 1991). In two dimensions, the dimensionless conductance $\tilde{g}(L) = \Delta E(L)/\delta E(L)$, which is usually taken as the scaling variable, is proportional to $\sigma(L)$, so no difficulties arise in choosing the correct scaling variable. $\tilde{g}$ is often called the Thouless number.

In the numerical work we proceed as follows. For each realization, we calculate the eigenvalues for cyclic boundary conditions and for modified cyclic boundary conditions in one direction. For modified boundary conditions, matrix elements that connect opposite lattice sides have been multiplied by a factor $(1 - \eta)$, with $\eta = 1/100$.

This strategy is similar to the one we applied to the quantum percolation problem (Koslowski and von Niessen 1990, 1991). Whereas for the quantum percolation problem a weak coupling scheme has been used for cyclic boundary conditions, the weak decoupling scheme described above conserves the topology of the lattice and allows the introduction of cyclic boundary conditions. Using this small decoupling, eigenvalue crossings are avoided, which usually lead to difficulties in the analysis of data within the framework of the TEL method. The Thouless number for the weak decoupling case will be denoted by g. It differs from the strong decoupling Thouless number $\tilde{g}$ only by a constant factor, not affecting its scaling behaviour. Whenever $g(L)$ increases with increasing system size L, i.e. the function $\beta(L) = \mathrm{d}\ln g/\mathrm{d}\ln L$ is larger than zero, the corresponding eigenstates are extended. If $g(L)$ decreases with increasing lattice size, i.e. the function $\beta(L) = \mathrm{d}\ln g/\mathrm{d}\ln L$ is smaller than zero, the corresponding eigenstates are localized. This interpretation is the same as in the scaling theory of localization (Abrahams *et al* 1979). Assuming an exponential behaviour of the conductance for localized states

$$g(L) \propto \exp(-L/L_{\mathrm{loc}}) \tag{5}$$

the localization length L_{loc} can be easily computed.

For the large matrix diagonalizations, we used a Lanczos algorithm (Lanczos 1950, Cullum and Willoughby 1985). It is ideally suited for large sparse matrix calculations, if just eigenvalues, but no eigenvectors are required.

3. Results and discussion

We have studied the effects of topological disorder for $p = 0.2$, $p = 0.4$ and $p = 0.8$. Calculations have been performed on systems with a length L of 20, 30, 40 and 50 R_0, corresponding to a maximum number of 2375 sites. The number of realizations for each p and L value is listed in table 1. p is dimensionless, $4V$ has been chosen as the unit of energy, R_0 as the unit of length.

Table 1. Number of realizations used in the TEL analysis for the continuous random network and the relaxed version (CRN-MC).

		$p = 0.2$	$p = 0.4$	$p = 0.8$
CRN	$L = 20$	904	1015	1285
	$L = 30$	173	197	262
	$L = 40$	55	62	82
	$L = 50$	23	26	33
CRN-MC	$L = 20$	688	771	938
	$L = 30$	129	145	177
	$L = 40$	41	46	56
	$L = 50$	17	19	23

Figure 2 shows a series of plots required for the TEL analysis of localization properties. They correspond to the simple tight-binding Hamiltonian (1). The energy spectrum has been divided into energy bins of width 0.045. Within each energy bin, the behaviour of $-\ln g$ with increasing lattice size is plotted from the left. Intervals

containing localized states are marked with an L. For all values of p, localized states can be observed at the upper band edge, whereas the lower band edge is not effected by topological disorder. The part of the spectrum containing localized states is increasing with increasing disorder, the mobility edge gradually moves into the interior part of the band. However, it should be noted that the major part of the spectrum is dominated by extended states even at large disorder p. This is the major difference to models such as quantum percolation or the Anderson model. Values for the mobility edges and the upper band edges are listed in table 2. Inverse localization lengths range from 0.029 ± 0.005 to 0.13 ± 0.02 for $p = 0.4$ and from 0.042 ± 0.004 to 0.36 ± 0.05 for $p = 0.8$, continuously increasing from the mobility edge to the band edge. For $p = 0.2$, the localization length equals 0.055 ± 0.008 in the single interval containing localized states.

Table 2. Upper (E_u) and lower (E_l) band edges, mobility edges (E_c) and optical energy (E_{op}) for the CRN and the relaxed CRN (CRN-MC).

		$p = 0.2$	$p = 0.4$	$p = 0.8$
CRN	E_c	0.97	0.88	0.65
	E_{op}	0.90	0.80	0.60
	E_u	0.98	0.95	0.88
CRN-MC	E_c^l	−1.08	−0.97	−0.81
	E_l	−1.40	≈ -1.5	< -1.5
	E_c^u	0.78	0.73	0.62
	E_u	0.95	0.86	0.81

Localization at the upper band edge can be explained by the picture of bond frustration (Singh 1981, Cohen 1983). At the upper band edge, the wave function has to be antibonding, it has to alternate when going from one lattice site to another. This is only possible for structures that contain rings with an even number of atoms. Whenever an odd ring is introduced, at least one bond of that ring has to be frustrated. The creation of frustrated bonds leads to a significant degree of disorder, which causes localization of those states most sensitive to this type of disorder. According to Singh (1981) and Cohen (1983), there exists a characteristic energy for topologically disordered systems, called the optical energy

$$E_{op} = (1 - 4\nu/Z) \tag{6}$$

where ν is the minimum number of frustrated bonds, divided by the total number of sites. Each vacancy introduces two frustrated bonds, connecting two pairs of atoms. As only one out of four atoms can be eliminated, equation (6) leads to

$$E_{op} = (1 - p/2). \tag{7}$$

As required by Singh (1983), the optical energy serves as a lower boundary for the mobility edge.

The density of states (DOS) of the tight-binding Hamiltonian is shown in figure 3. For all values of p, the lower band edge equals the band edge of the crystalline system, $E = -1.0$. The part of the spectrum containing localized states has been shaded. At $p = 0.2$, the density of states looks similar to the DOS for a finite-ordered

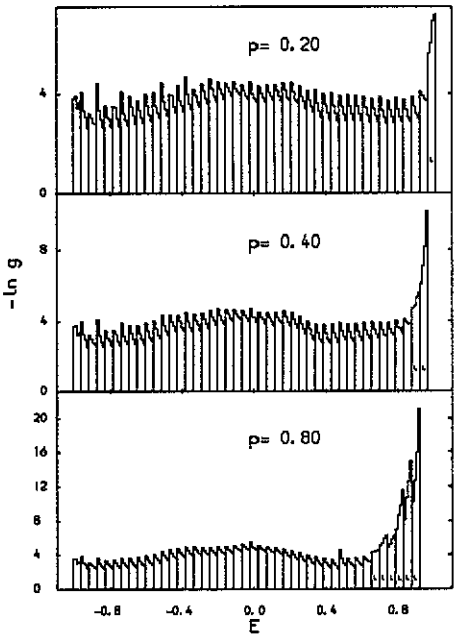

Figure 2. Negative logarithm of the Thouless number as a function of energy for the CRN. Energy in units of $\frac{1}{4}V$.

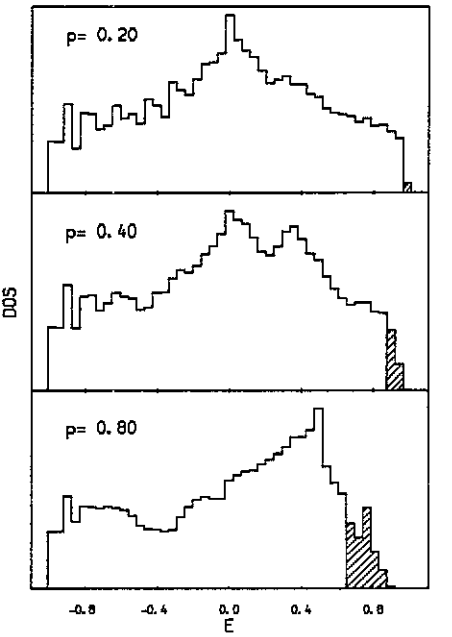

Figure 3. Density of states for the CRN. Energy in units of $\frac{1}{4}V$, density of states in arbitrary units. Localized parts have been shaded.

system. There is maximum DOS at $E = 0$, which turns into a singularity for an infinite-ordered system. Only at the upper band edge, a very small region of localized states exists. The upper band edge is moving to smaller values of E with increasing disorder, but in a much smoother way than the mobility edge does. So the part of the spectrum containing localized states is increasing with increasing disorder.

The same analysis has been performed for a relaxed CRN. Its electronic properties are calculated from an extended Hückel Hamiltonian with an interaction given by equation (3). The TEL plots are shown in figure 4, the width of an energy bin equals 0.053. The same vacancy concentrations have been used for both the tight-binding and the extended Hückel Hamiltonian. At the upper band edge, localization properties are similar to those of the simple tight-binding Hamiltonian. There is a region dominated by localized states, moving to values of lower energy with increasing p. In contrast to the behaviour observed for the tight-binding Hamiltonian, the total width of the localized part of the spectrum does not depend on the vacancy concentration. In addition to localization at the upper band edge, localization which is induced by off-diagonal disorder can be observed at the lower band edge. It is restricted to a part of the spectrum which shows a small density of states, in qualitative agreement with mean field theories of localization (Winn and Logan 1990). Upper band inverse localization lengths range from 0.014 ± 0.005 to 0.44 ± 0.04 for $p = 0.2$, from 0.063 ± 0.005 to 0.31 ± 0.02 for $p = 0.4$ and from 0.020 ± 0.007 to 0.26 ± 0.04 for $p = 0.8$, covering a smaller length scale than the tight-binding localization lengths. In this model, the optical energy is no longer a lower boundary for the mobility edge. The density of states for the extended Hückel Hamiltonian is shown in figure 5. Localized

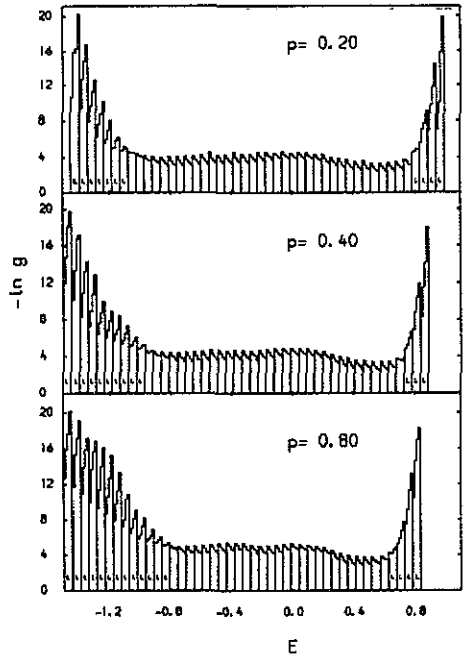

Figure 4. Negative logarithm of the Thouless number as a function of energy for the relaxed CRN. Energy in units of V_0.

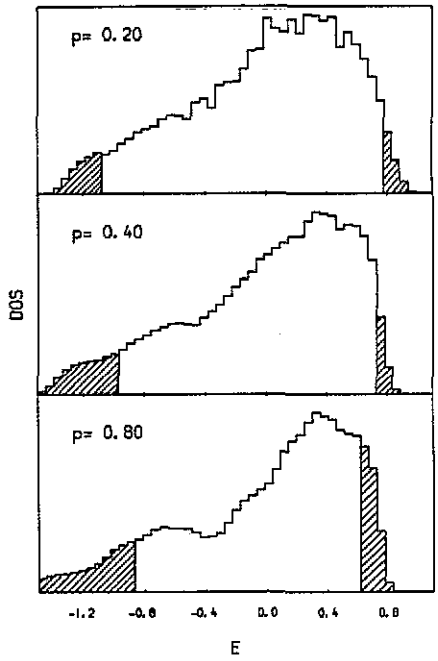

Figure 5. Density of states for the relaxed CRN. Energy in units of V_0, density of states in arbitrary units.

parts of the spectrum have been shaded.

In two dimensions, variable range hopping can be described similar to Mott's $T^{-1/4}$ law (Mott 1968). In the hopping regime, the conductivity is expected to obey a $T^{-1/3}$ law (Hamilton 1972):

$$\sigma = A\exp(-B/T^{1/3}). \tag{8}$$

The exponential factor B depends on the density of states and the localization length at the Fermi level. Thus, B can be calculated by the scheme presented above, giving direct connection to a hypothetical experiment, if the Fermi energy lies within the region of localized states.

According to the scaling theory of localization, no extended states should occur for any amount of disorder in two-dimensional systems (Abrahams *et al* 1979). Whereas this behaviour is in good agreement with numerical calculations for the Anderson model (MacKinnon and Kramer 1983), there are doubts whether the scaling theory holds for system with off-diagonal disorder like the quantum percolation model (Meir *et al* 1989, Koslowski and von Niessen 1990) The localization behaviour for CRNs clearly is in contrast to the scaling theory. Extended states do not disappear even at very large vacancy concentrations. On the other hand, weak localization may occur on a length scale much larger than the maximum system length used in this calculation, which cannot be detected with the TEL method.

As mentioned above, the creation of a continuous random network using the vacancy model can be easily extended to three-dimensional systems. Actually, it was designed to create a CRN on the diamond lattice (Duffy *et al* 1974). The creation

of five-membered rings on a diamond lattice will lead to much less ring tension than induced by the quite rigid three-membered rings on the square lattice. So a Keating relaxation will lead to a much sharper distribution of bond angles with a single maximum. Extended Hückel calculations have already been performed successfully on clusters of amorphous silicon and hydrogenated amorphous silicon (Han and Dai 1989). They can be easily applied to a CRN, followed by a TEL analysis of the eigenvalues. No prediction of localization properties on CRNs in three dimensions can be made from the calculations described above. Localization will be suppressed by a high Euclidean dimension on one side. On the other side, it will be enhanced by the participation of p orbitals at the band edges (Singh 1981), because interaction integrals including p orbitals are more sensitive to a variation of dihedral angles, leading to large variation in these integrals. Numerical work is in progress to resolve this problem.

4. Conclusions

In this article, we have reported numerical results for localization induced by disorder on a continuous random network. A simple tight-binding model and a Hamiltonian with off-diagonal disorder have been used to calculate the localization behaviour of electronic states. Localization properties like mobility edges or localization lengths significantly depend on the model Hamiltonian used. Off-diagonal order leads to lower-band localization, a feature not predicted by the simple tight-binding Hamiltonian. We think that the choice of the appropriate model Hamiltonian is much more important for the calculation of localization properties than it is for a band structure calculation.

Acknowledgments

We thank the computing centre of the TU Braunschweig, where the calculations have been performed on an IBM 3090/600 computer. Financial support of the Deutsche Forschungsgemeinschaft (DFG) and partial support from the Fonds der Chemischen Industrie are gratefully acknowledged.

References

Abrahams E, Anderson P W, Licciardello D C and Ramakrishnan T V 1979 *Phys. Rev. Lett.* **42** 673
Anderson P W 1958 *Phys. Rev.* **109** 1492
Ando T 1988 *Anderson Localization* ed T Ando and H Fukuyama (Berlin: Springer)
—— 1989 *Phys. Rev.* B **40** 5325
Cohen M H 1983 *Topological Disorder in Condensed Matter* ed F Yonezawa and T Ninomiya (Berlin: Springer)
Cullum J K and Willoughby R K 1985 *Lanczos Algorithms for Large Symmetric Eigenvalue Problems, vol I Theory, vol II Programs* (Boston: Birkhäuser)
Duffy M G, Boudreaux D S and Polk D E 1974 *J. Non-Cryst. Solids* **15** 435
Edwards J T and Thouless D J 1972 *J. Phys. C: Solid State Phys.* **5** 807
Elliott S R 1983 *Physics of Amorphous Materials* (London: Longman)
Gibbons M K, Logan D E and Madden P E 1988 *Phys. Rev.* B **38** 7292
Hamilton E M 1972 *Phil. Mag.* **26** 1043

Han S and Dai G 1989 *Chin. J. Semicond.* **10** 587
Hoffmann R 1963 *J. Chem. Phys.* **39** 1397
Keating P W 1966 *Phys. Rev.* **145** 637
Koslowski Th and von Niessen W 1990 *Phys. Rev.* B **42** 10342
—— 1992 *Phys. Rev.* B **44** 9926
Lanczos C 1950 *J. Res. NBS* B **45** 225
Licciardello D C and Thouless D J 1975 *J. Phys. C: Solid State Phys.* **8** 4157
—— 1978 *J. Phys. C: Solid State Phys.* **11** 925
MacKinnon A and Kramer B 1983 *Z. Phys.* B **53** 1
Meir Y, Aharony A and Harris A B 1989 *Europhys. Lett.* **10** 275
Mott N F 1968 *J. Non-Cryst. Solids* **1** 1
Mott N F and Davis E 1971 *Electronic Processes in Non-Crystalline Solids* (London:Oxford University Press)
Polk D E 1971 *J. Non-Cryst. Solids* **5** 365
Singh J 1981 *Phys. Rev.* B **23** 4156
Soukoulis C M, Economou E N and Grest G S 1987 *Phys. Rev.* B **36** 8649
Winn M D and Logan D E 1990 *Phys. Chem. Liq.* **22** 11
Ziman J M 1969 *J. Phys. C: Solid State Phys.* **2** 1230